SECURITY CLASSIFICATION OF THIS PAGE (When Data Entered)

# REPORT DOCUMENTATION PAGE

READ INSTRUCTIONS BEFORE COMPLETING FORM

| | |
|---|---|
| 1. REPORT NUMBER: R83-920015-F | 2. GOVT ACCESSION NO. |
| 3. RECIPIENT'S CATALOG NUMBER | |
| 4. TITLE (and Subtitle): FURTHER DEVELOPMENT OF A TRANSONIC CASCADE ANALYSIS | 5. TYPE OF REPORT & PERIOD COVERED: Final Report, 10 Aug 1982 - 10 Aug 1983 |
| | 6. PERFORMING ORG. REPORT NUMBER |
| 7. AUTHOR(s): S.J. Shamroth, R.-J. Yang, H. McDonald | 8. CONTRACT OR GRANT NUMBER(s): N00019-82-C-0248 |
| 9. PERFORMING ORGANIZATION NAME AND ADDRESS: Scientific Research Associates, Inc., P.O. Box 498, Glastonbury, CT 06033 | 10. PROGRAM ELEMENT, PROJECT, TASK AREA & WORK UNIT NUMBERS |
| 11. CONTROLLING OFFICE NAME AND ADDRESS: Naval Air Systems Command, Code AIR-310, Washington, DC 20361 | 12. REPORT DATE: September 1983 |
| | 13. NUMBER OF PAGES: 46 |
| 14. MONITORING AGENCY NAME & ADDRESS (if different from Controlling Office): DCASMA - Hartford, 96 Murphy Rd., Hartford, CT 06114 | 15. SECURITY CLASS. (of this report): Unclassified |
| | 15a. DECLASSIFICATION/DOWNGRADING SCHEDULE |

16. DISTRIBUTION STATEMENT (of this Report)

APPROVED FOR PUBLIC RELEASE
DISTRIBUTION UNLIMITED

17. DISTRIBUTION STATEMENT (of the abstract entered in Block 20, if different from Report)

18. SUPPLEMENTARY NOTES

19. KEY WORDS (Continue on reverse side if necessary and identify by block number)

Transonic Cascades
Navier-Stokes
Turbines
Compressors

20. ABSTRACT (Continue on reverse side if necessary and identify by block number)

A compressible, time-dependent solution of the Navier-Stokes equations is obtained for both compressor and turbine cascade configurations in subsonic and transonic flows. The analysis uses the Briley-McDonald consistently split linearized block implicit (LBI) procedure to solve the governing equations. Comparisons with measured data are presented for both turbulence energy and mixing length turbulence models. In addition, consideration is given to boundary conditions for the cascade flutter problem.

DD FORM 1 JAN 73 1473 EDITION OF 1 NOV 65 IS OBSOLETE

Unclassified
SECURITY CLASSIFICATION OF THIS PAGE (When Data Entered)

Report R83-920015-F



# FURTHER DEVELOPMENT OF A TRANSONIC CASCADE ANALYSIS

S. J. Shamroth, R.-J. Yang and H. McDonald
Scientific Research Associates, Inc.
Glastonbury, CT 06033

September 1983

Final Report
Prepared Under Contract N00019-82-C-0298

Prepared for
NAVAL AIR SYSTEMS COMMAND
Department of Navy

TABLE OF CONTENTS

# I. INTRODUCTION

The present report represents the latest portion of an ongoing effort aimed at the development of a Navier-Stokes analysis for the general steady or unsteady cascade flow field problem. Although the two-dimensional cascade analysis represents a simplified version of the actual three-dimensional flow field which includes end wall effects, the two-dimensional problem gives significant insight into the cascade flow field and obviously is a necessary first step in developing a three-dimensional analysis. Hence, cascade analyses of various types have been a subject of high interest in recent years. Among the analyses being pursued are inviscid analyses (e.g. Refs. 1 and 2), inviscid analyses with boundary layer corrections (e.g. Ref. 3) and Navier-Stokes analyses (e.g. Ref. 4 and 5). Each of these approaches are viable under certain circumstances. For example, inviscid analyses can give good predictions of the blade pressure distribution for conditions where the effect of viscous phenomena upon the blade pressure distribution remains small. However, inviscid analyses require some method of assuming airfoil circulation to obtain a unique flow solution. In general this specification is straight-forward for sharp trailing edged blades in steady flow where the Kutta-Joukowski condition serves to specify circulation. However, in cases where the trailing edge is rounded or the flow is unsteady or trailing edge separation occurs specification of a proper condition is not clear. Finally,

---


1. Farrel, C. and Adamczyk, J.: Full Potential Solution of Transonic Quasi-3-D Flow Through a Cascade Using Artificial Compressibility. ASME Paper 81-GT-70, 1981.

2. Casper, J.R., Hobbs, D.E. and Davis, R.L.: The Calculation of Two-Dimensional Compressible Potential Flow in Cascades Using Finite Area Techniques. AIAA Paper 79-0077, 1977.

3. Hansen, E.C., Serovy, G.K. and Sockol, P.M.: Axial Flow Compressor Turning Angle and Loss by Inviscid-Viscous Interaction Blade-to-Blade Computation, Journal of Engineering for Power, Vol. 102, 1980.

4. Shamroth, S.J. and McDonald, H.: An Assessment of an Ensemble-Averaged Navier-Stokes Calculation Procedure for Cascade Flow Fields. Scientific Research Associates Report R82-920011-F, 1982.

5. Shamroth, S.J., McDonald, H. and Briley, W.R.: Prediction of Cascade Flow Fields Using the Averaged Navier-Stokes Equations. To be published in ASME Journal of Engineering for Power.

inviscid methods obviously cannot give either heat transfer or viscous loss estimates. Nevertheless, despite these inherent limitations, inviscid analyses are valuable for the prediction of blade pressure distributions for flows having little viscous displacement effect and a clearly applicable Kutta condition.

Some limitations of inviscid analyses can be relieved by combining an inviscid flow calculation procedure for the pressure distribution with a viscous flow boundary layer development in either a strong interaction or a weak interaction mode. A recent example of a combined viscous-inviscid procedure is the work of Hansen, Serovy and Sockol (Ref. 3). In cases where the viscous displacement effect has an insignificant or only small effect on the actual blade pressure distribution, an inviscid calculation can be made to obtain the pressure distribution and a boundary layer calculation then made to obtain heat transfer and loss effects. However, in many cases the viscous displacement effect may significantly alter the pressure distribution. Such cases are found when boundary layers become thick or separate or in transonic flow where the local pressure distribution and shock location become very sensitive to small change in the effective passage area. In these cases a strong interaction solution is required to account for the mutual effects of the viscous boundary layer and the nominally inviscid core flow.

A strong interaction analysis may take the form of either a forward marching procedure or a global iteration. For regions where the outer nominally inviscid flow is supersonic (and thus described by hyperbolic equations) a solution can be spatially forward marched in the nominally streamwise direction with the inviscid and viscous regions coupled on a station-by-station basis. The chief difficulty with this approach is the stiff nature of the coupled sets of equations which is manifested in the appearance of physically unrealistic branching solutions. In regions where the outer flow is subsonic, the outer flow equations are elliptic in nature and in these regions forward marching in the streamwise spatial direction is not possible and consequently a series of viscous and inviscid calculations must be performed in which each corrects the other in a global manner. Problems with interaction solutions become particularly severe in transonic flows where both subsonic and supersonic nominally inviscid regions are present and where small viscous displacement effects may have a major effect on the blade pressure distribution and shock location. A final difficulty with the interactive approach occurs when boundary layer separation appears. Here with an imposed

pressure field, the usual steady state boundary layer equations are unstable when solved as an initial value problem in space in regions of reversed flow. However, the equations can be marched in space by suppressing the streamwise convection term in the separated region (Ref. 6). Although this approximation allows the solution to be marched through separation, the approximation becomes progressively more inaccurate as the extent of the separation zone or the magnitude of either the normal or the back flow velocities become large. Thus, calculated flow details which may be important (such as heat transfer at reattachment) may have significant error when separation is present and such an interactive analysis is used. Other schemes have and are being developed which solve the interaction problem without encountering an instability by either changing the problem to initial value in time or iteration space. Nonetheless the resulting solutions still retain the approximations of the boundary layer equations and the inviscid flow. However, as with inviscid flow solutions, combined viscous and inviscid solutions remain a valuable tool for those classes of cascade problems where the approximations adopted are valid.

The final procedure currently available is the solution of full ensemble-averaged Navier-Stokes equations. Such an analysis has been applied to a variety of cascade flow fields by Shamroth, Gibeling and McDonald (Ref. 7) Shamroth, McDonald and Briley (Refs. 5, 8-10) and by Shamroth and McDonald (Ref. 4). The use of the full Navier-Stokes equations for the cascade problem

---


6. Rehyner, T. and Flugge-Lotz, I.: The Interaction of Shock Waves with a Laminar Boundary Layer. International Journal of Nonlinear Mechanics, Vol. 3, 1968.

7. Shamroth, S.J., Gibeling, H.J. and McDonald, H.: A Navier-Stokes Solution of Laminar and Turbulent Flow Through a Cascade of Airfoils. AIAA Paper No. 80-1426, 1980. (Also, SRA Report R79-920004-F, 1982.)

8. Shamroth, S.J., McDonald, H. and Briley, W.R.: A Navier-Stokes Solution for Transonic Flow Through a Cascade. SRA Report R82-920007-F, 1982.

9. Shamroth, S.J., McDonald, H. and Briley, W.R.: Application of a Navier-Stokes Analysis to Transonic Cascade Flow Fields. ASME Paper 82-GT-235, 1982.

10. McDonald, H., Shamroth, S.J. and Briley, W.R.: Transonic Flows with Viscous Effects, Transonic Shock and Multi-Dimensional Flows: Advances in Scientific Computing. Academic Press, New York, 1982.

allows use of a single set of equations for the entire flow field and thus removes the need for an interaction analysis to couple different equation descriptions for different flow regions. The analysis simultaneously predicts both the blade pressure distribution and viscous and heat transfer effects.

The initial effort in the present ongoing program is detailed in Ref. 7 where a constructive cascade coordinate system was combined with a Navier-Stokes calculation procedure to compute subsonic flow fields in a simple cascade of unstaggered NACA 0012 airfoils. The coordinate system generation process was based upon that of Eiseman (Ref. 11). The calculation procedure used was the linearized block implicit (LBI) method of Briley and McDonald (Ref. 12) which obtains a solution by marching the assumed initial flow field in time until a steady state is reached. Although the cases chosen were geometrically simple cascade flows, the convergence of the solution to steady state in a relatively few number of time steps ($\sim 150$) showed the practicality of the approach.

The approach was extended to more realistic cascade flow fields in Ref. 8 where calculations for a cascade of Sanz airfoils were made. The coordinate system generation code developed by Eiseman was modified by Kim and Shamroth (Ref. 13) to allow specification of more general cascades than were previously allowed. This new generalized code was used to generate the Sanz cascade coordinate system. In addition, under this effort, a study was made of possible artificial dissipation formulations. Based upon results obtained for a model one-dimensional flow problem containing a shock wave, a second order artificial dissipation approach was judged to be an effective method of suppressing spatial oscillations resulting from a central difference representation of derivatives. This same technique was then applied to transonic flow through a cascade of Sanz airfoils. It was demonstrated that

---

11. Eiseman, P.R.: A Coordinate System for a Viscous Transonic Cascade Analysis. Journal of Computational Physics, Vol. 26, March 1978, pp. 307-338.

12. Briley, W.R. and McDonald, H.: Solution of the Multi-Dimensional Compressible Navier-Stokes Equations by a Generalized Implicit Method. Journal of Computational Physics, Vol. 24, 1977.

13. Kim, Y.-N. and Shamroth, S.J.: Revised Coordinate Generation Program for a Cascade of Arbitrary Shaped Airfoils. SRA Report 81-1, 1981.

second order artificial dissipation could be added to the governing equations in a manner which would suppress spurious spatial oscillations but not significantly contaminate the solution.

Finally, in Ref. 4 the same procedure was used to calculate flow through turbine and compressor cascade where experimental data was available. The turbine cascade chosen was that of Turner (Ref. 14) and the compressor cascade that of Stephens and Hobbs (Refs. 15 and 16). Both subsonic and transonic flow conditions were considered and comparisons between calculation and measurement were made for both pressure distributions and velocity profiles. In general the comparison for blade pressure distribution was judged to be good (see Ref. 4 for details), however some discrepancy appeared in the boundary layer profiles. The present effort focuses upon a further study of the boundary layer profile comparison as well as consideration of boundary conditions to be applied for blade movement corresponding to small forced vibrations.

---

14. Turner, A.B.: Local Heat Transfer Measurements on a Gas Turbine Blade. Journal of Mechanical Engineering Sciences, Vol. 13, 1971.

15. Stephens, H.E. and Hobbs, D.E.: Design and Performance of Supercritical Airfoils for Axial Flow Compressors. Pratt and Whitney Aircraft Report FR11455, 1979.

16. Hobbs, D.E., Wagner, J.H., Dannenhoffer, J.F., Dring, R.P.: Wake Experiment and Modelling for Fore and Aft-loaded Compressor Cascade. Pratt and Whitney Aircraft Report FR13514, 1980.

## II. ANALYSIS

The present analysis is based upon a solution of the ensemble-averaged Navier-Stokes equations using the linearized block implicit method of Briley and McDonald (Ref. 12). The equations are solved in a constructive coordinate system (Ref. 4) with density and the Cartesian velocity components being taken as dependent variables. The application of the LBI method to the cascade flow field problem has been discussed in some detail in Refs. 4, and 7-10. However, for completeness it will be repeated here along with a brief discussion of the coordinate system and governing equations.

### Coordinate System

An important component of the cascade analysis is the cascade coordinate system. Any coordinate system used in the analysis should satisfy conditions of (i) generality, (ii) smoothness, (iii) resolvability and (iv) allow easy application of boundary conditions. Obviously, a coordinate system must be sufficiently general to allow application to a wide class of problems of interest if it is to be practical. The metric data associated with the coordinate system must be sufficiently smooth so that the variation from grid point to grid point does not lead to a numerical solution dominated by metric coefficient truncation error. It should be noted that this requirement differs from the requirement of the existence of a specified number of transformation derivatives. The coordinate system must resolve flow regions where rapid flow field changes occur. Finally, coordinates should allow accurate implementation of boundary conditions; for the cascade this requirement is equivalent to the requirement that the metric coefficients be continuous across the periodic lines where periodic boundary conditions are to be applied.

To date, several types of coordinate systems are available. These include (i) solutions based upon a conformal transformation, (ii) solutions based upon solution of a Poisson equation (e.g. Ref. 17), and constructive systems. The present approach uses a constructive system based originally upon the approach of Eiseman (Ref. 11) which has been revised by Kim and Shamroth (Ref. 13). A

---

17. Thompson, J.F., Thames, F.C. and Mastin, C.W.: Boundary Fitted Curvilinear Coordinate Systems for Solution of Partial Differential Equations on Fields Containing Any Number of Arbitrary Two-Dimensional Bodies. NASA CR-2729, July 1977.

computer generated plot of the coordinate system for the Jose Sanz diffusion cascade is shown in Fig. 1. As can be seen in Fig. 1, the coordinate systems consist of two sets of curves; the $\xi$ = constant curves such as FG or HI and the $\eta$ = constant curves such as ABCD or A'ED'. In constructing the coordinate system care must be taken that metric data remains smooth from grid point to grid point, and adequate resolution is obtained both near the blade surface and in the leading edge region. Details of the construction process are given in Appendix A.

## Governing Equations

The present effort solves the time-dependent compressible Navier-Stokes equations to predict the cascade flow field. If the computational spatial coordinates are $\xi$ and $\eta$ where

$$\xi = \xi(x,y,t) \qquad \eta = \eta(x,y,t) \qquad \tau = t \tag{1}$$

then the continuity equation, the x-component of the momentum equation and the y-component of the momentum equation are written as

$$\frac{\partial W}{\partial \tau} + \xi_t \frac{\partial W}{\partial \xi} + \xi_x \frac{\partial F}{\partial \xi} + \xi_y \frac{\partial G}{\partial \xi} + \eta_t \frac{\partial W}{\partial \eta} + \eta_x \frac{\partial F}{\partial \eta} + \eta_y \frac{\partial G}{\partial \eta} = \frac{1}{Re}\left[ \xi_x \frac{\partial F_1}{\partial \xi} + \eta_x \frac{\partial F_1}{\partial \eta} + \xi_y \frac{\partial G_1}{\partial \xi} + \eta_y \frac{\partial G_1}{\partial \eta} \right] \tag{2}$$

where

$$\begin{pmatrix} \rho \\ \rho u \\ \rho v \end{pmatrix}, \quad F = \begin{pmatrix} \rho u \\ \rho u^2 + p \\ \rho uv \end{pmatrix}, \quad G = \begin{pmatrix} \rho v \\ \rho uv \\ \rho v^2 + p \end{pmatrix} \quad F_1 = \begin{pmatrix} 0 \\ \tau_{xx} \\ \tau_{xy} \end{pmatrix} \quad G_1 = \begin{pmatrix} 0 \\ \tau_{xy} \\ \tau_{yy} \end{pmatrix} \tag{3}$$

$$D = \xi_x \eta_y - \xi_y \eta_x$$

In Eqs. (1-3) x and y are Cartesian coordinates, t is time, u and v are velocity components, $\rho$ is density, p is pressure, and $\tau_{ij}$ is the stress

tensor and Re is the Reynolds number. This formulation is termed the quasi-linear form and has been used successfully for a number of cascade and airfoil calculations [7-10, 18, 19] for both laminar and turbulent flow in the subsonic and transonic regimes.

The dependent variables chosen for the present formulation are the density, $\rho$, and the velocity components, u and w. Although the code does contain an energy equation and calculations have been made with an energy equation, most calculations have been run with the assumption $T^\circ$, the stagnation temperature, equals a constant. With this assumption, the pressure is related to the velocity and density by

$$P = \rho R \left( T^\circ - \frac{(u^2 + v^2)}{2C_p} \right) \tag{4}$$

## Numerical Procedure

The numerical procedure used to solve the governing equations is a consistently split linearized block implicit (LBI) scheme originally developed by Briley and McDonald (Ref. 12). A conceptually similar scheme has been developed for two-dimensional MHD problems by Lindemuth and Killeen (Ref. 20). The procedure is discussed in detail in Refs. 12 and 21. The method can be briefly outlined as follows: the governing equations are replaced by an implicit time difference approximation, optionally a backward difference or

---

18. Shamroth, S.J. and Gibeling, H.J.: A Compressible Solution of the Navier-Stokes Equations for Turbulent Flow about an Airfoil. NASA CR-3183, 1979. (Also, AIAA Paper 79-1543).

19. Shamroth, S.J. and Gibeling, H.J.: Analysis of Turbulent Flow about an Isolated Airfoil Using a Time-Dependent Navier-Stokes Procedure. AGARD CP 296, 1980.

20. Lindemuth, I. and Killeen, J.: Alternating Direction Implilcit Techniques for Two-Dimensional Magnetohydrodynamic Calculations. Journal of Computational Physics, 13, 1973.

21. Briley, W.R., and McDonald, H.: On the Structure and Use of Linearized Block Implicit Schemes. Journal of Computational Physics, Vol. 34, 1980.

Crank-Nicolson scheme. Terms involving nonlinearities at the implicit time level are linearized by Taylor expansion in time about the solution at the known time level, and spatial difference approximations are introduced. The result is a system of multi-dimensional coupled (but linear) difference equations for the dependent variables at the unknown or implicit time level. To solve these difference equations, the Douglas-Gunn (Ref. 22) procedure for generating alternating-direction implicit (ADI) schemes as perturbations of fundamental implicit difference schemes is introduced in its natural extension to systems of partial differential equations. This technique leads to systems of coupled linear difference equations having narrow block-banded matrix structures which can be solved efficiently by standard block-elimination methods.

The method centers around the use of a formal linearization technique adapted for the integration of initial-value problems. The linearization technique, which requires an implicit solution procedure, permits the solution of coupled nonlinear equations in one space dimension (to the requisite degree of accuracy) by a one-step noniterative scheme. Since no iteration is required to compute the solution for a single time step, and since only moderate effort is required for solution of the implicit difference equations, the method is computationally efficient; this efficiency is retained for multi-dimensional problems by using what might be termed block ADI techniques. The method is also economical in terms of computer storage, in its present form requiring only two time-levels of storage for each dependent variable. Furthermore, the block ADI technique reduces multi-dimensional problems to sequences of calculations which are one-dimensional in the sense that easily-solved narrow block-banded matrices associated with one-dimensional rows of grid points are produced. A more detailed discussion of the solution procedure as discussed by Briley, Buggeln and McDonald (Ref. 23) is given in the Appendix B.

### Artificial Dissipation

Since the calculations of interest are often at high Reynolds numbers

22. Douglas, J. and Gunn, J.E.: A General Formulation of Alternating Direction Methods. Numerische Math., Vol. 6, 1964, pp. 428-453.

23. Briley, W.R., Buggeln, R.C. and McDonald, H.: Computation of Laminar and Turbulent Flow in 90 Degree Square Duct and Pipe Bends Using the Navier-Stokes Equations. SRA Report R82-920009-F, 1982.

typical of normal turbomachinery applications, it is necessary to add "artificial dissipation" terms to suppress spatial oscillations associated with central spatial differences approximations. This can be done via a dissipative spatial difference formulation (e.g., one-sided difference approximations for first derivatives) or by explicitly adding an additional dissipative type term. For the Navier-Stokes equations, the present authors favor the latter approach since when an additional term is explicitly added, the physical approximation being made is usually clearer than when dissipative mechanisms are contained within numerical truncation errors, and further, explicit addition of an artificial dissipation term allows greater control over the amount of non-physical dissipation being added. Obviously, the most desirable technique would add only enough dissipative mechanism to suppress oscillations without deteriorating solution accuracy. Various methods of adding artificial dissipation were investigated in Ref. 8, and these were evaluated in the context of a model one-dimensional problem containing a shock with a known analytic solution (one-dimensional flow with heat transfer). The methods which were considered included second-order dissipation, fourth-order dissipation and pressure dissipation techniques.

As a result of this investigation, it was concluded that a second-order anisotropic artificial dissipation formulation suppressed spatial oscillations without impacting adversely on accuracy and could be used to capture shocks successfully. In this formulation, the terms

$$\rho^{n-1} d_x \frac{\partial^2 \phi}{\partial x^2} , \quad \rho^{n-1} d_y \frac{\partial^2 \phi}{\partial y^2}$$

are added to the governing equations where $\phi$ = u, v and $\rho$ for the x-momentum, y-momentum and continuity equations, respectively. The exponent n is zero for the continuity equation and unity for the momentum equations. The dissipation coefficient $d_x$ is determined as follows. The general equation has an x-direction convective term of the form $a\partial\phi/\partial x$ and an x-direction diffusion term of the form $\partial(b\partial\phi/\partial x)/\partial x$. The diffusive term is expanded

$$\partial(b\,\partial\phi/\partial x)/dx = b\,\partial^2\phi/\partial x^2 + \partial b/\partial x\,\partial\phi/\partial x \qquad (5)$$

and then a local cell Reynolds number $Re_{\Delta x}$ is defined for the x-direction by

$$Re_{\Delta x} = \left|a - \partial b/\partial x\right|\Delta x/b \qquad (6)$$

where b is the total or effective viscosity including both laminar and turbulent contributions, and $\Delta x$ is the grid spacing. The dissipation coefficient $d_x$ is non-negative and is chosen as the larger of zero and the local quantity $b\,(\sigma_x Re_{\Delta x}-1)$. The dissipation parameter $\sigma_x$ is a specified constant and represents the inverse of the cell Reynolds number below which no artificial dissipation is added. The dissipation coefficient $d_y$ is evaluated in an analogous manner and is based on the local cell Reynolds number $Re_{\Delta y}$ and grid spacing $\Delta y$ for the y-direction and the specified parameter $\sigma_y$. It should be noted that recently calculations have been run with artificial dissipation added in the conservative form $\partial(\rho^{n-1}d_x\partial\phi/\partial x)/\partial x$ and no significant difference between the forms was noted for the particular flows examined.

The question arises as to the values of $\sigma_x$ and $\sigma_y$ which should be chosen. This was assessed both through the model problem (Ref. 8), and through calculations for a Jose Sanz compressor cascade (Refs. 4 and 8). These results indicated that values of $\sigma = .5$ which correspond to a cell Reynolds number 2 limitation would severely damp physical variations. However, when $\sigma$ was set in the range $.025 \leq \sigma \leq 0.05$, which correspond to a cell Reynolds number range between 40 and 20, spurious spatial oscillations were damped with no significant change in the calculated results as $\sigma$ was varied in this range. Further, as discussed in Refs. 4 and 7-10, the results obtained showed good agreement with data. This has since been confirmed at several other studies at Scientific Research Associates such as two- and three-dimensional transonic

nozzle flows (Ref. 24) where a maximum acceptable value of $\sigma = 0.10$ has been noted for most problems. Therefore, based upon this past experience, second-order damping is applied with $\sigma$ taken as 0.05.

## Boundary Conditions

The authors' experience in solving Navier-Stokes equations has indicated the important role boundary conditions play in determining accurate solutions and rapid numerical convergence. The boundary conditions used in the present calculations follow the suggestion of Briley and McDonald (Ref. 25) which specifies upstream total pressure and downstream static pressure conditions. For the cascade system shown in Fig. 1, AB and CD are periodic boundaries and periodic conditions are set here.

Specification of upstream and downstream conditions is somewhat more difficult. For an isolated cascade, boundary conditions for the differential equations may be known at both upstream infinity and downstream infinity. However, since computation economics argues for placing grid points in the vicinity of the cascade and minimizing the number of grid points far from the cascade, the upstream and downstream computational boundaries should be set as close to the cascade as is practical. In addition, with the particular body-fitted coordinates used, as the upstream boundary moves further upstream, the angle between pseudo-radial and pseudo-azimuthal coordinate lines becomes smaller. Decreasing the coordinate angle causes the coordinate system to

24. Liu, N.S., Shamroth, S.J. and McDonald, H.: Numerical Solution of the Navier-Stokes Equations for Compressible Turbulent Two/Three Dimensional Flows in the Terminal Shock Region of an Inlet/Diffuser. AIAA Paper 83-1892, 1983.

25. Briley, W.R. and McDonald, H.: Computation of Three-Dimensional Horseshoe Vortex Flow Using the Navier-Stokes Equations. Seventh International Conference on Numerical Methods in Fluid Dynamics, 1980.

to become less well-conditioned, increases truncation error (Ref. 26), and increases the role of cross-derivative terms in the equations. All of these characteristics could be detrimental to the present numerical procedure and, therefore, they also argue for placing the upstream boundary as close to the cascade as possible. However, when the upstream boundary is placed close to the cascade, most flow function conditions on the boundary will not be known, since these will have been changed from values at infinity by the presence of the cascade.

In the present approach, the suggestion of Ref. 25 is followed which sets total pressure on boundary BC (see Fig. 1). Unless boundary BC is very far upstream, the flow velocity along this boundary will not be equal to the velocity at upstream infinity since some inviscid deceleration will have occurred. However, as long as the boundary is upstream of the region of any significant viscous or shock phenomena, the total pressure on this boundary will be equal to the total pressure at upstream infinity. Hence, total pressure is an appropriate boundary condition realistically modeling the desired flow condition. In addition to specifying upstream total pressure, it is necessary to specify the inlet flow angle. In the present calculation, a value was assumed constant on the upstream boundary at a specified value. The third condition set on the upstream boundary concerns the density and a zero density derivative at this boundary was specified as a numerical treatment of the boundary. The downstream boundary was treated by setting a constant static pressure as a boundary condition, and by setting second derivatives of both velocity components equal to zero at this location. In the present application, a constant static pressure was set at downstream infinity, and hence it is assumed that the downstream boundary is located in a region where pressure is uniform.

Both the upstrem and downstream boundaries have boundary conditions associated with them which are nonlinear functions of the dependent variables. These are the specifications of total pressure on the upstream boundary and static pressure on the downstream boundary. These nonlinear boudnary conditions are linearized in the same manner as the governing equations (via a Taylor expansion of the dependent variable in time), and then solved implicitly

26. Mastin, C.W.: Error Induced by Coordinate Systems, Numerical Grid Generation, J.F. Thompson, Ed., Elsevier Publishing, New York, 1982.

along with the interior point equations. The final boundary conditions to be considered are the conditions along the blade surface. Here no-slip and no through-flow conditions were applied leading to a specification of zero velocity on the surface. An inviscid transverse momentum equation was applied on the surface leading to a boundary condition approximation of zero transverse pressure gradient being applied.

## III. CURRENT EFFORTS

Current efforts pursued under the present contract consisted of three parts: computer code speed-up, turbulence model studies and consideration of time-dependent, forced vibration-type boundary conditions. These are now discussed in detail.

### Code Efficiency

The original cascade computer code was a very general code which was written for maximum flexibility. In this regard, equations, boundary conditions, dependent variables, coordinate systems, difference schemes, etc. could be easily changed and the choice of equations and boundary conditions were made by the user. For example, user specified input determined if an energy equation was solved or constant total enthalpy assumed, the choice of two- or three-dimensional flow was made via input and the choice of constructive versus quasi-linear equations form was made by input. In addition, several options such as reacting flow, two-phase flow, cylindrical polar geometry, etc. which are not relevant to the cascade problem were available. Although this generality is very desirable from the viewpoint of deck development and deck flexibility, it does require a price in terms of computer run time. Therefore, as a first item under the present effort the existing code was modified to increase deck efficiency.

The modifications still allow considerable generality such as choice of equations, choice of boundary conditions, arbtrary geometry, conservative or quasi-linear equation form, etc. However, certain portions of the code not required for cascade calculations such as cylindrical polar coordinates and reacting flow were eliminated. In addition, the original matrix inverter was replaced by a more efficient procedure and the computational coordinates were assumed to be equally spaced. It should be noted that since the computational

coordinates are general non-physical coordinates, see Eq. (1), this does not place a restriction on nonuniform meshes in physical space and, in fact, all cases run to date were run with equally spaced computational coordinates.

The resulting modification decreased computer run time by approximately 55 per cent and, therefore, allows considerable additional computer runs for a given computer budget. The new code requires approximately 0.0034 secs per grid point per time step for a code operating with an out-of-core option. If the code were run completely in core, this time would reduce to approximately 0.0025 secs. It is estimated that an additional factor of 2 saving could be obtained without loss of generality with further code restructuring. Obviously, even further savings are available with code vectorization and/or modifications restricting generality.

## Turbulence Model Modifications

One major focus of the present effort was further consideration, and possible modification, of turbulence models in the existing computer program. At the beginning of the present phase, the code allowed for either of two turbulence models; these were a mixing length model and a turbulence energy - algebraic length scale model.

In the mixing length model, the turbulent viscosity is related to the mean strain via a mixing length, $\ell$, such that

$$\mu_T = \rho \ell^2 \left[ \left( \frac{\partial u_i}{\partial x_j} + \frac{\partial u_j}{\partial x_i} \right) \frac{\partial u_i}{\partial x_j} \right]^{1/2} \tag{7}$$

where $\mu_T$ is the turbulent viscosity, $\rho$ is the density, $\ell$ is the mixing length, $u_i$ is the $i^{th}$ velocity component and $x_i$ is the $i^{th}$ Cartesian direction. Summation is implied for the repeated indices. The question now arises as to specification of $\ell$. For the region upstream of the trailing edge the mixing length is specified in the usual boundary layer manner; i.e.

$$\ell = \kappa y \left(1 - e^{-y^+/27}\right) \qquad \ell \leq \ell_{max} \tag{8}$$

where $\kappa$ is the von Karman constant and $y^+$ is the dimensionless normal coordinate, $yu_\tau/\nu$. In boundary layer analysis $\ell_{max}$ is usually taken as $0.09\delta$ where $\delta$ is the boundary layer thickness taken as the location where $u/u_e = 0.99$. However, this definition of $\delta$ assumes the existence of an outer flow where the velocity $u_e$ is independent of distance from the wall at a given streamwise station, i.e., it assumes $u_e$ is only a function of the streamwise coordinate. Although a boundary layer calculation will yield solutions in which u approaches $u_e$ asymptotically at distances far from the solid no-slip surface, Navier-Stokes solutions for cascade flow fields do not in general predict a region where u asymptotes to a constant value. Furthermore, measurements of the flow also show no such region to exist in general. Obviously, a proper choice of $\delta$ for the Navier-Stokes cascade analysis is not straight forward. Calculations made in Refs. 4 and 7-9 have set the boundary layer thickness by first determining $u_{max}$, the maximum streamwise velocity, at a given station and then setting $\delta$ via

$$\delta = 2.0\, y_{(u/u_{max} = k_1)} \tag{9}$$

;i.e., $\delta$ was taken as twice the distance for which $u/u_{max} = k_1$. Two values of $k_1$ were used in the previous efforts; these were 0.80 and 0.95. Although the predicted pressure distribution was relatively insensitive to choice, the boundary layer development did depend upon the choice of $k_1$.

The model used in the wake is also a mixing length model in which the mixing length was made proportional to the wake height, $\delta$, and a linear of growth of $\delta$ with distance was assumed based upon the classical free jet boundary results (e.g. [27]). With the free jet boundary growth assumption

$$\delta = \left(\delta_{ps} + \delta_{ss}\right) + (.2)(x - x_{TE}) \tag{10}$$

where $\delta_{ps}$ and $\delta_{ss}$ are the pressure and suction surface trailing edge boundary layer thickness and $x_{te}$ is the trailing edge location. The mixing length, $\ell$, was taken as $0.2\delta$.

---

27. Schlichting, H.: Boundary Layer Theory, McGraw Hill, New York, 1960.

Using this formulation, calculated profiles were compared with measured profiles for the data of Hobbs, Wagner, Dannenhoffer and Dring (Ref. 16). In Ref. 16, boundary layer profiles were measured on both the suction and pressure surfaces in the vicinity of the blade trailing edge region. In this regard, it should be noted that the resulting boundary layers on both surfaces are subjected to strong favorable pressure gradients followed by adverse pressure gradients with these effects being considerably more pronounced on the suction surface. Therefore, the boundary layer at the trailing edge has a history of both strong favorable and adverse pressure gradients and its profile depends both upon this history and the transition point location.

The comparisons of Ref. 4 showed very good agreement between the measured profiles and the calculated profiles on the pressure surface. On the suction surface agreement, although acceptable, was not as good. In addition, the choice of the variable, $k_1$, (see Eq. (9)) could significantly change the calculated profile. Therefore, a more detailed study of the turbulence model was warranted.

As a first step in the re-evaluation, the code was used to calculate a constant pressure turbulent boundary and the resulting profile is compared to data compilations in Fig. 2. As can be seen, the predicted profile is in good agreement with the compiled data. In this calculation

$$\delta = 2.0 y_{(u/u_{max} = 0.8)} \tag{11}$$

These results in conjunction with the boundary layer profiles presented in Ref. 4 indicate reasonable agreement between calculation and experiment can be obtained using the mixing length model with a proper choice of $\delta$. Obviously, these results are preliminary and not conclusive. To be made conclusive, considerably more comparisons with data would be required.

The major obstacle in using the mixing length model resides in the specification of the length scale $\delta$, and it may be advantageous to utilize a turbulence model which does not require specification for a length scale. One model which fits this requirement is the so-called k-$\varepsilon$ model which solves governing equations for the turbulence energy, k, and the turbulent dissipation, $\varepsilon$, and then calculates $\mu_T$ from these quantities. The equations governing the development of k and $\varepsilon$ have been given by several authors

(e.g. Launder and Spalding Ref. 28). One form in which the equations may be expressed is

$$\frac{\partial \rho k}{\partial t} + \frac{\partial \rho u k}{\partial x} + \frac{\partial \rho u k}{\partial y} = \frac{\partial}{\partial x_k}\left[\left(\mu + \frac{\mu_T}{\sigma_k}\right)\frac{\partial k}{\partial x_k}\right] + \mu_T\left(\frac{\partial u_i}{\partial x_k} + \frac{\partial u_k}{\partial x_i}\right)\frac{\partial u_i}{\partial x_k} - \rho\epsilon + D \qquad (12)$$

$$\frac{\partial \rho \epsilon}{\partial t} + \frac{\partial \rho u \epsilon}{\partial x} + \frac{\partial \rho v \epsilon}{\partial y} = \frac{\partial}{\partial x_j}\left[\left(\mu + \frac{\mu_T}{\sigma_k}\right)\frac{\partial \epsilon}{\partial x_j}\right] + C_1\frac{\epsilon}{k}\mu_T\left(\frac{\partial u_i}{\partial x_k} + \frac{\partial u_k}{\partial x_i}\right)\frac{\partial u_i}{\partial x_k} - C_2\frac{\rho\epsilon^2}{k} + E \qquad (13)$$

$$\mu_T = \rho C_\mu k^2/\epsilon \qquad (14)$$

where D, E, $C_1$, $C_2$, $C_\mu$, $\sigma_k$ and $\sigma_\varepsilon$ are functions which vary from particuar model to model. A recent comparison of several k-ε models has been given by Patel, Rodi and Scheuerer (Ref. 29). In the present analysis the

---

28. Launder, B.E. and Spalding, D.B.: The Numerical Computation of Turbulent Flows, Computer Methods in Applied Mechanics and Engineering, Vol. 3, 1974, pp. 269-287.

29. Patel, V.C., Rodi, W. and Scheurer, G.: Evaluation of Turbulence Models for Near Wall and Low Reynolds Number Flows. Third Symposium on Turbulent Shear Flow. University of California, Davis, 1981.

following functional forms were set

$$
\begin{aligned}
\sigma_\epsilon &= 1.3 \\
\sigma_k &= 1.0 \\
C_1 &= 1.43 \\
C_\mu &= 0.09 \exp\left[-2.5/(1 + R_\tau/50)\right] \\
C_2 &= 1.92\left[1.0 - 0.3 \exp(-R_\tau^2)\right]
\end{aligned}
\qquad (15)
$$

$$
D = -2\mu \frac{\partial k^{1/2}}{\partial x_j} \frac{\partial k^{1/2}}{\partial x_j}
$$

$$
E = -2\mu\mu_T \left( \frac{\partial^2 u_i}{\partial x_k \, \partial x_k} \right)^2
$$

This corresponds to equations given by Launder and Spalding in Ref. 28. Further discussion of the equations is given in some detail in Refs. 28 and 29.

A similar Navier-Stokes code using the same equations and the same algorithm has been run at SRA under an Army Research Office program to calculate a transonic shock boundary layer interaction in a constant radius tube (Ref. 30), and these results are repeated here since they demonstrate a

---

30. McDonald, H., Roscoe, D.V., Gibeling, H.J. and Shamroth, S.J.: Progress Report for Contract DAAG29-80-C-0082, December 1981.

transonic calculation. The case considered had supersonic inflow in a straight tube with a near normal shock resulting from the specified back pressure. The calculation was run to correspond with data of Mateer, Brosh and Viegas for both a mixing length and a k-ε model (Ref. 31). A comparison of calculated and measured pressure distributions is given in Fig. 3. As can be seen, agreement is very good. A comparison for the predicted and measured streamwise velocity profiles is presented in Fig. 4. Both calculations show good agreement with data although the mixing length calculation is in slightly better agreement with data than is the k-ε calculation. These results give encouragement for the use of the k-ε model in non-simple viscous flow fields where a mixing length application may not suffice and give impetus to the inclusion of thse models in the cascade deck. However, as discussed in Ref. 29, k-ε models are not always satisfactory even in simple boundary layers so the approach is taken with some caution.

Under the present effort, Eqs. (12) and (13) have been incorporated into the Navier-Stokes cascade code and the subsonic cascade configuration of Hobbs, et al (Ref. 16) has been recalculated. A plot of predicted and measured blade pressure distribution is shown in Fig. 5 which compares measured data with mixing length and k-ε calculations. As can be seen, both calculated pressure distributions are nearly the same and agree well with the measured data.

Predictions of the boundary layer profile are given in Figs. 6-9. Although the calculations presented in Ref. 4 give good agreement with data, they were run for a value of $k_1 = 0.95$ in Eq. (9) which appears to be unrealistically large. Therefore, the mixing length calculations were rerun for k = 0.90 which appears to be a more reasonable value. Calculations were also run for fully turbulent and forced transition situations. It should be recalled that when the mixing length model is used, the flow is considered turbulent throughout with the turbulent viscosity over the airfoil set by Eqs. (7) through (11). Since the maximum length scale is determined by the boundary layer thickness, the turbulent viscosity is small in the leading

---

31. Mateer, G.G., Brock, A. and Viegas, J.R.: A Normal Shock-Wave Turbulent Boundary Layer Interaction at Transonic Speeds. AIAA Paper 76-161, 1976.

edge region and the flow is essentially laminar here. However, a turbulent viscosity is calculated throughout; this calculation is termed the fully turbulent calculation. Alternatively, the calculation can be run in a mode where the turbulent viscosity is set to zero upstream of a specified streamwise location. This is termed the forced transition model. Similarly when the k-ε model is utilized, it predicts a turbulent viscosity throughout the flow. In certain regions, this viscosity may be small and in these regions the flow will be laminar. However, a calculation can be made whereby the turbulent viscosity is set to zero upstream of a specified location. This latter mode is termed the forced transition mode.

Predictions of the pressure surface boundary layer are given in Figs. 6 and 7. Figs. 6 and 7 compare fully turbulent and free transition models for the mixing length and k-ε models respectively. As can be seen, agreement in all cases is good. In all cases of forced transition, laminar flow was imposed for $s/c < 0.18$ which is the location where transition steps were placed in the experiment.

Predictions of the suction surface boundary layer is given in Figs. 8 and 9. The mixing length calculations are given in Fig. 8 where as shown the forced transition calculation is in much better agreement with the data than is the fully turbulent calculation. This calculation, in conjunction with other calculations, indicate that the calculated suction surface boundary layer profile is sensitive both to the chosen value of $k_1$ and the assumption of free or forced transition. The major effect of requiring laminar flow for $s/c < .18$ was to maintain a thinner boundary layer at the beginning of adverse pressure gradient regions. This effect was then magnified as the boundary layer was subjected to the strong adverse pressure gradient and the results are shown in Fig. 8.

Calculations made with the k-ε model are given in Fig. 9. As can be seen, differences again appear between the fully turbulent and forced transition model. However, the effect of requiring laminar flow for $s/c < .18$, is not as pronounced in this case and both calculations predict boundary layers which are thicker than those measured experimentally. It should be noted that the k-ε equations do contain low Reynolds number effects. These are incorporated in the model via the functional forms $C_\mu$ and $C_2$ and may account for near wall and/or transitional effects. Although these models have been used with some

success for relaminarizing boundary layers (Ref. 32), their application to boundary layers in arbitrary pressure gradients has found only modest success (e.g. Ref. 29), and they have yet to be successfully applied to boundary layers in forward transition. In regard to the forced transition k-ε calculation this was run with the k-ε equation solved throughout the entire flow field. The results indicate that for compressor cascade flow fields a model capable of predicting transition accurately may be required to obtain accurate suction surface velocity profile predictions. Therefore, based upon these results two possible approaches for further turbulence model work appear viable. The first would be to concentrate upon application of the k-ε model to flows in forward transition. The second would investigate alternate k-ε type models such as those discussed in Ref. 29.

## Unsteady Boundary Conditions

To date, the Navier-Stokes cascade analysis has focused upon steady or unsteady flows through a cascade of stationary airfoils. Another important problem area is that of flow through a cascade in which the blades are moving relative one to another. This problem arises in connection with free-vibration or flutter phenomena in the compressor or turbine stages of modern turbomachinery or engine configurations. Early approaches to this problem were based upon classical linear analyses which assumed flat plate blades at zero incidence to the mean flow (e.g. Ref. 33). Although these procedures can give useful insight into the fluid dynamic process, they are obviously limited by their assumptions of zero mean incidence, zero thickness and camber and inviscid flow. More recent analyses although confined to inviscid flows have removed the zero mean incidence and flat geometry restrictions (e.g. Ref. 34). Although these still treat the time-dependent flow as a linear perturbation

---


32. Jones, W.P. and Launder, B.E.: Some Properties of Sink Flow Turbulent Boundary Layers, Journal of Fluid Mechanics, Vol. 46, 1972, pp. 337-351.

33. Whitehed, D.S.: Vibration and Sound Generation in a Cascade of Flat Plates in Subsonic Flow. Aeronautical Research Council R and M 3685, 1970.

34. Verdon, J.M. and Caspar, J.R.: Development of an Unsteady Aerodynamic Analysis for Finite-Reflection Subsonic Cascades. NASA CR-3455, 1981.

from the mean flow, they represent a more general analysis.

Under the present effort, initial consideration was given to application of the Navier-Stokes cascade analysis to the oscillating cascade problem so as to reduce the inviscid and small perturbation assumptions. Since the present procedure solves the time-dependent equations in a general coordinate system which may be a function of time, the procedure is clearly applicable to the oscillating cascade problem. However, boundary condition specification presents a difficulty.

One approach in principle which is not practical would consider all N blades of an N-bladed cascade with the azimuthal coordinate of the cascade varying between 0° and 360°. Since the points at 0° and 360° are physically the same point, a true periodic boundary condition could be applied. Alternately an N-bladed recti-linear cascade could be considered. If N were large, then the flow in the middle passage might be relatively insensitive to the boundary conditions applied at stagnation lines and wake lines for blades 1 and N. Unfortunately, either of these options would be impractical due to the large number of grid points required and, therefore, an alternative formulation is sought whereby the flow in a given passage or between two adjacent flow periodic lines in the steady case represents the flow in any passage (or between any two adjacent flow periodic lines) in the cascade. Obviously, if the flow field is to exhibit such periodicity, the driving blade motion must exhibit a periodicity. The general type of blade motion can be given for the $m^{th}$ blade by

$$\begin{aligned} x_d &= \delta_x f_x(\omega_1 t + \phi_1 + m_1\sigma) \\ y_d &= \delta_y f_y(\omega_2 t + \phi_2 + m_2\sigma) \end{aligned} \tag{16}$$

where $x_d$ and $y_d$ are displacement of the blade from its mean position $\sigma$ is a constant interblade phase angle, and f represents a periodic function and $\delta_x$ and $\delta_y$ represent oscillation amplitudes. This represents a moving wave through the blade row.

Turning to Fig. 1, the problem can be illustrated by the question of what boundary conditions on boundaries BA and CD will represent the motion specified by Eq. (16) of all blades external to this portion of the flow field. Since a periodic solution with phase lag is sought, then the dependent variables on corresponding points of lines AB and CD must bear a periodic type relation. If the value of any dependent variable, $\Psi$, obtained for a steady solution is denoted $\psi$ and

$$(\psi_I) = \Psi - \psi \tag{17}$$

Then $\psi_G = \psi_L$ since these represent corresponding periodic points. For the unsteady case, the solution sought is one in which the disturbed variable, $(\psi_I)$ is periodic with a possible interblade phase lag between corresponding points; i.e. if

$$(\psi_I)_G = f(\omega t + \phi_G) \tag{18}$$

then

$$(\psi_I)_L = f(\omega t + \phi_L) = f(\omega t + \phi_G + \sigma)$$

The problem obviously arises as to the choice of the periodic function f and the phase angle $\phi_G$ which may be a function of the spatial coordinates. These must be determined from some other source as they are boundary conditions to the viscous problem. One possible method would determine f and $\phi_G$ from a small perterbation solution such as that of Ref. 34. For example, if the blade motion for blade m is given by

$$\begin{aligned} x_d &= 0 \\ y_d &= \epsilon_1 \cos(\omega t + m\sigma) \end{aligned} \tag{19}$$

where $\epsilon_1$, $\omega$ and $\sigma$ are specified and the inviscid, small perturbation solution for the dependent variable $\Psi$ at point G is

$$\Psi = \psi + (\psi_1)_G = \psi + \epsilon_2 \cos(\omega t + \phi_G) \tag{20}$$

then at point L

$$\Psi = \psi + (\psi_1)_L = \psi + \epsilon_2 \cos(\omega t + \phi_G - \sigma) \tag{21}$$

and a periodic type boundary condition of the type

$$\left[\Psi - \psi\right]_G \cos(\omega t + \phi_G - \sigma) = \left[\Psi - \psi\right]_L \cos(\omega t + \phi_G) \tag{22}$$

results. If $\phi_G$ is specified for each point on the periodic boundary, then Eq. (22) represents a possible boundary condition relating variables G and L. The existing Navier-Stokes cascade code has been extended to allow a boundary condition of the form of Eq. (22).

A second possible approach follows that of Erdos, Alzner and Kalben in their application of the Euler equations to cascade problem (Ref. 35). In this approach, the equations are solved in the passage region between points L' and G' where L' and G'' are periodic points in steady flow as are G' and L'' (see Fig. 1). In this approach, the dependent variables at G' are related to those at L'' at some earlier time depending upon interblade phase angle. Similarly, the dependent variables at L' are related to those at G''. With this approach, the second sweep equations which solve along lines F G' and M L' are solved with specified function boundary conditions. This approach will require some run time to establish the moving wave disturbance type flow. In addition, application of these boundary conditions may adversely affect stability. However, the formulation does represent a possible approach.

## CONCLUDING REMARKS

The present report represents continuation of an effort aimed at applying the Navier-Stokes equations to subsonic and transonic, turbulent cascade flow fields. During previous efforts, work focused upon development of a cascade computational coordinate system, calculation of laminar and turbulent

---

35. Erdos, J., Alzner, A. and Kalben, P.: Computation of Steady and Periodic Two-Dimensional Non-linear Transonic Flow Problems in Turbomachinery, (T.C. Adamson and M.F. Platzer, Editors), Hemisphere Publishing, Washington, 1977.

cascade flows, development of a shock capturing technique and comparison of calculated flow fields with data. Under the present effort, the computer code was revised to reduce run time, a turbulence energy-turbulence dissipation model was added to the code, a calculation was run to convergence with this new turbulence model and consideration given to the forced blade vibration problem. The revised code runs more than twice as fast as the original code with little loss of code flexibility. It is estimated that further restructuring would reduce run time by an additional factor of two without loss of generality. The calculation run with the turbulence energy-turbulence dissipation model reached convergence with no problem. The predicted surface pressure distribution agreed well with data, however, discrepancies were present between the calculated and measured suction surface boundary layer profiles. One possible source of discrepancy is the laminar to turbulent transition process and future work should focus upon this phenomenon. Finally, consideration has been given to the problem of boundary conditions for the forced vibration problem.

## REFERENCES


1. Farrel, C. and Adamczyk, J.: Full Potential Solution of Transonic Quasi-3-D Flow Through a Cascade Using Artificial Compressibility. ASME Paper 81-GT-70, 1981.

2. Caspar, J.R., Hobbs, D.E. and Davis, R.L.: The Calculation of Two-Dimensional Compressible Potential Flow in Cascades Using Finite Area Techniques. AIAA Paper 79-0077, 1977.

3. Hansen, E.C., Serovy, G.K. and Sockol, P.M.: Axial Flow Compressor Turning Angle and Loss by Inviscid-Viscous Interaction Blade-to-Blade Computation, Journal of Engineering for Power, Vol. 102, 1980.

4. Shamroth, S.J. and McDonald, H.: An Assessment of an Ensemble-Averaged Navier-Stokes Calculation Procedure for Cascade Flow Fields. Scientific Research Associates Report R82-920011-F, 1982.

5. Shamroth, S.J., McDonald, H. and Briley, W.R.: Prediction of Cascade Flow Fields Using the Averaged Navier-Stokes Equations. To be published in ASME Journal of Engineering for Power.

6. Rehyner, T. and Flugge-Lotz, I.: The Interaction of Shock Waves with a Laminar Boundary Layer. International Journal of Nonlinear Mechanics, Vol. 3, 1968.

7. Shamroth, S.J., Gibeling, H.J. and McDonald, H.: A Navier-Stokes Solution for Laminar and Turbulent Flow Through a Cascade of Airfoils. AIAA Paper No. 80-1426, 1980. (Also, SRA Report R79-920004-F).

8. Shamroth, S.J., McDonald, H. and Briley, W.R.: A Navier-Stokes Solution for Transonic Flow Through a Cascade. SRA Report R81-920007-F, 1982.

9. Shamroth, S.J., McDonald, H. and Briley, W.R.: Application of a Navier-Stokes Analysis to Transonic Cascade Flow Fields. ASME Paper 82-GT-235, 1982.

10. McDonald, H., Shamroth, S.J. and Briley, W.R.: Transonic Flows with Viscous Effects, Transonic Shock and Multi-Dimensional Flows: Advances in Scientific Computing. Academic Press, New York, 1982.

11. Eiseman, P.R.: A Coordinate System for a Viscous Transonic Cascade Analysis. Journal of Computational Physics, Vol. 26, March 1978, pp. 307-338.

12. Briley, W.R. and McDonald, H.: Solution of the Multi-Dimensional Compressible Navier-Stokes Equations by a Generalized Implicit Method. Journal of Computational Physics, Vol. 24, 1977.

13. Kim, Y.-N. and Shamroth, S.J.: Revised Coordinate Generation Program for a Cascade of Arbitrary Shaped Airfoils. SRA Report 81-1, 1981.

14. Turner, A.B.: Local Heat Transfer Measurementes on a Gas Turbine Blade. Journal of Mechanical Engineering Sciences, Vol. 13, 1971.

15. Stephens, H.E. and Hobbs, D.E.: Design and Performance of Supercritical Airfoils for Axial Flow Compressors. Pratt and Whitney Aircraft Report FR11455, 1979.

16. Hobbs, D.E., Wagner, J.H., Dannenhoffer, J.F., Dring, R.P.: Wake Experiment and Modelling for Fore and Aft-loaded Compressor Cascade. Pratt and Whitney Aircraft Report FR13514, 1980.

17. Thompson, J.F., Thames, F.C. and Mastin, C.W.: Boundary Fitted Curvilinear Coordinate Systems for Solution of Partial Differential Equations on Fields Containing Any Number of Arbitrary Two-Dimensional Bodies. NASA CR-2729, July 1977.

18. Shamroth, S.J. and Gibeling, H.J.: A Compressible Solution of the Navier-Stokes Equations for Turbulent Flow about an Airfoil. NASA CR-3183, 1979. (Also, AIAA Paper 79-1543).

19. Shamroth, S.J. and Gibling, H.J.: Analysis of Turbulent Flow About an Isolated Airfoil Using a Time-Dependent Navier-Stokes Procedure. Paper presented at AGARD Specialists Meeting on Boundary Layer Effects on Unsteady Airload, Aix-en-Provence, France, September 1980.

20. Lindemuth, I. and Killeen, J.: Alternating Direction Implicit Techniques for Two-Dimensional Magnetohydrodynamic Calculations. Journal of Computational Physics, 13, 1973.

21. Briley, W.R. and McDonald, H.: On the Structure and Use of Linearized Block Implicit Schemes. Journal of Computational Physics, Vol. 34, 1980.

22. Douglas, J. and Gunn, J.E.: A General Formulation of Alternating Direction Methods. Numerische Math., Vol. 6, 1964, pp. 428-453.

23. Briley, W.R., Buggeln, R.C. and McDonald, H.: Computation of Laminar and Turbulent Flow in 90 Degree Square Duct and Pipe Bends Using the Navier-Stokes Equations. SRA Report R82-920009-F, 1982.

24. Liu, N.-S., Shamroth, S.J. and McDonald, H.: Numerical Solution of the Navier-Stokes Equations for Compressible Turbulent Two/Three Dimensional Flows in the Terminal Shock Region of an Inlet/Diffuser. AIAA Paper 83-1892, 1983.

25. Briley, W.R. and McDonald, H.: Computation of Three-Dimensional Horseshoe Vortex Flow Using the Navier-Stokes Equations. Seventh International Conference on Numerical Methods in Fluid Dynamics, 1980.

26. Mastin, C.W.: Error Induced by Coordinate Systems, Numerical Grid Generation, J.F. Thompson, Ed., Elsevier Publishing, New York, 1982.

27. Schlichting, H.: Boundary Layer Theory, McGraw Hill, New York, 1960.

28. Launder, B.E. and Spalding, D.B.: The Numerical Computation of Turbulent Flows - Computer Methods in Applied Mechanics and Engineering, Vol. 3, 1974, pp. 269-287.

29. Patel, V.C., Rodi, W. and Scheurer, G.: Evaluation of Turbulence Models for Near Wall and Low Reynolds Number Flows. Third Symposium on Turbulent Shear Flow. University of California, Davis, 1981.

30. McDonald, H., Roscoe, D.V., Gibeling, H.J. and Shamroth, S.J.: Progress Report for Contract DAAG29-80-C-0082, December 1981.

31. Mateer, G.G., Brock, A. and Viegas, J.R.: A Normal Shock-Wave Turbulent Boundary Layer Interaction at Transonic Speeds. AIAA Paper 76-161, 1976.

32. Jones, W.P. and Launder, B.E.: Some Properties of Sink Flow Turbulent Boundary Layers, Journal of Fluid Mechanics, Vol. 46, 1972, pp. 337-351.

33. Whitehead, D.S.: Vibration and Sound Generation in a Cascade of Flat Plates in Subsonic Flow. Aeronautical Research Council R and M 3685, 1970.

34. Verdon, J.M. and Caspar, J.R.: Development of an Unsteady Aerodynamic Analysis for Finite-Reflection Subsonic Cascades. NASA CR-3455, 1981.

35. Erdos, J., Alzner, A. and Kalben, P.: Computation of Steady and Periodic Two-Dimensional Non-linear Transonic Flow Problems in Turbomachinery, (T.C. Adamson and M.F. Platzer, Editors), Hemisphere Publishing, Washington, 1977.

36. Beam, R.M. and Warming, R.F.: An Implicit Factored Scheme for Compressible Navier-Stokes Equations. AIAA Journal, Vol. 16, 1978.

37. Beam, R.M. and Warming, R.F.: An Implicit Finite Difference Algorithm for Hyperbolic Systems in Conservation Law Form. Journal of Computational Physics,Vol. 22, 1976.

38. Beam, R.M. and Warming, R.F.: Alternating Direction Implicit Methods for Parabolic Equations with a Mixed Derivative. SIAM J. Sci. Stat. Comp., Vol. 1, 1980.

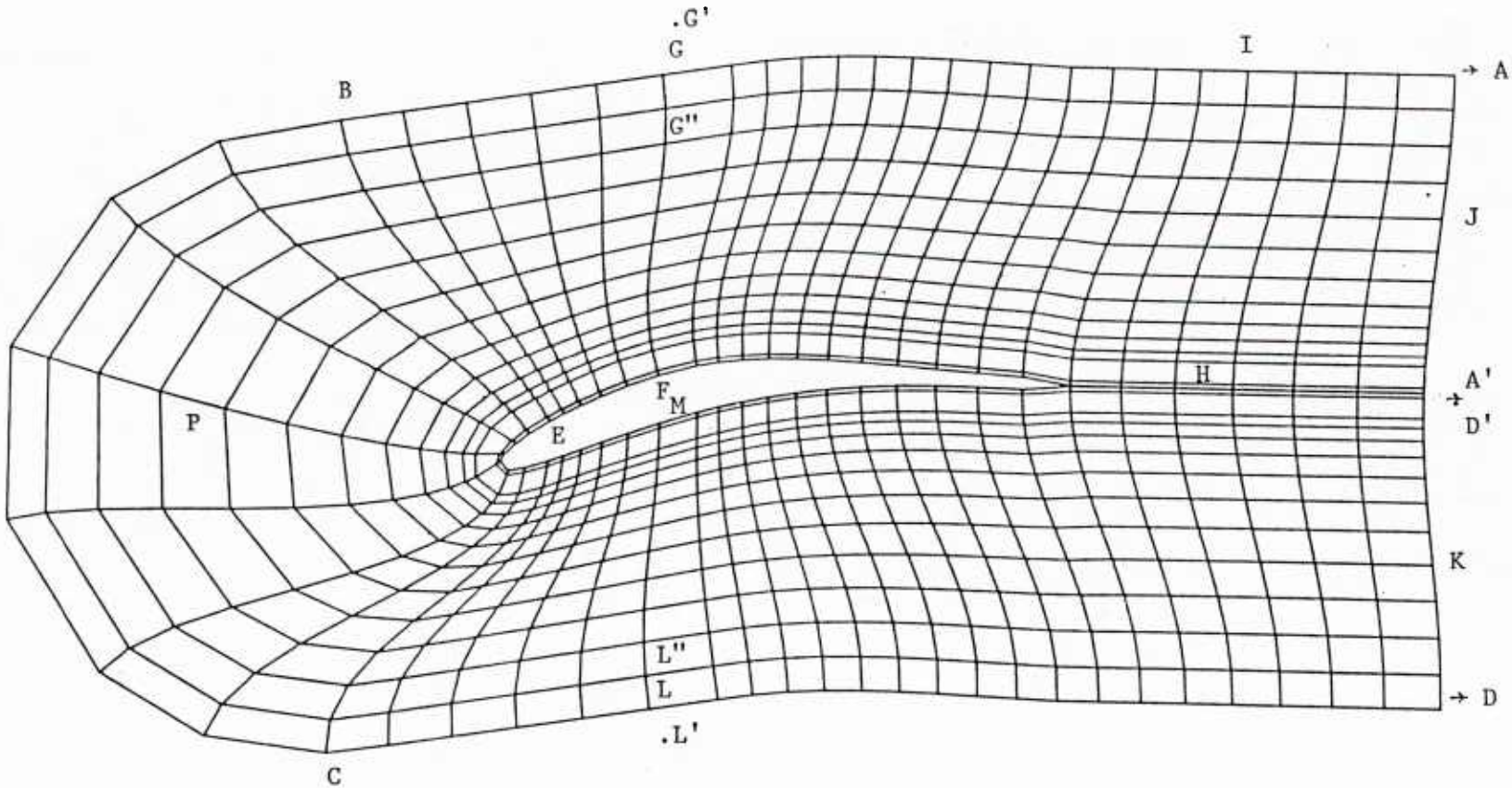


Fig. 1 - Cascade coordinate grid - all grid points not included.

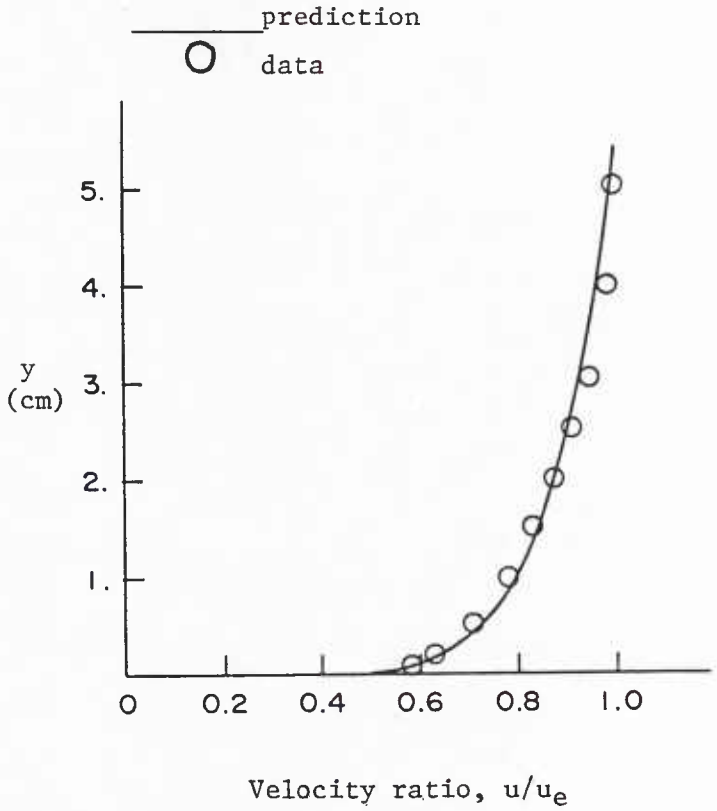


Fig. 2 - Boundary layer profile (Coles and Hirst, 1968 Stanford Conference, Vol. 2, Compiled Data, ID-1400, x = 2.887m)

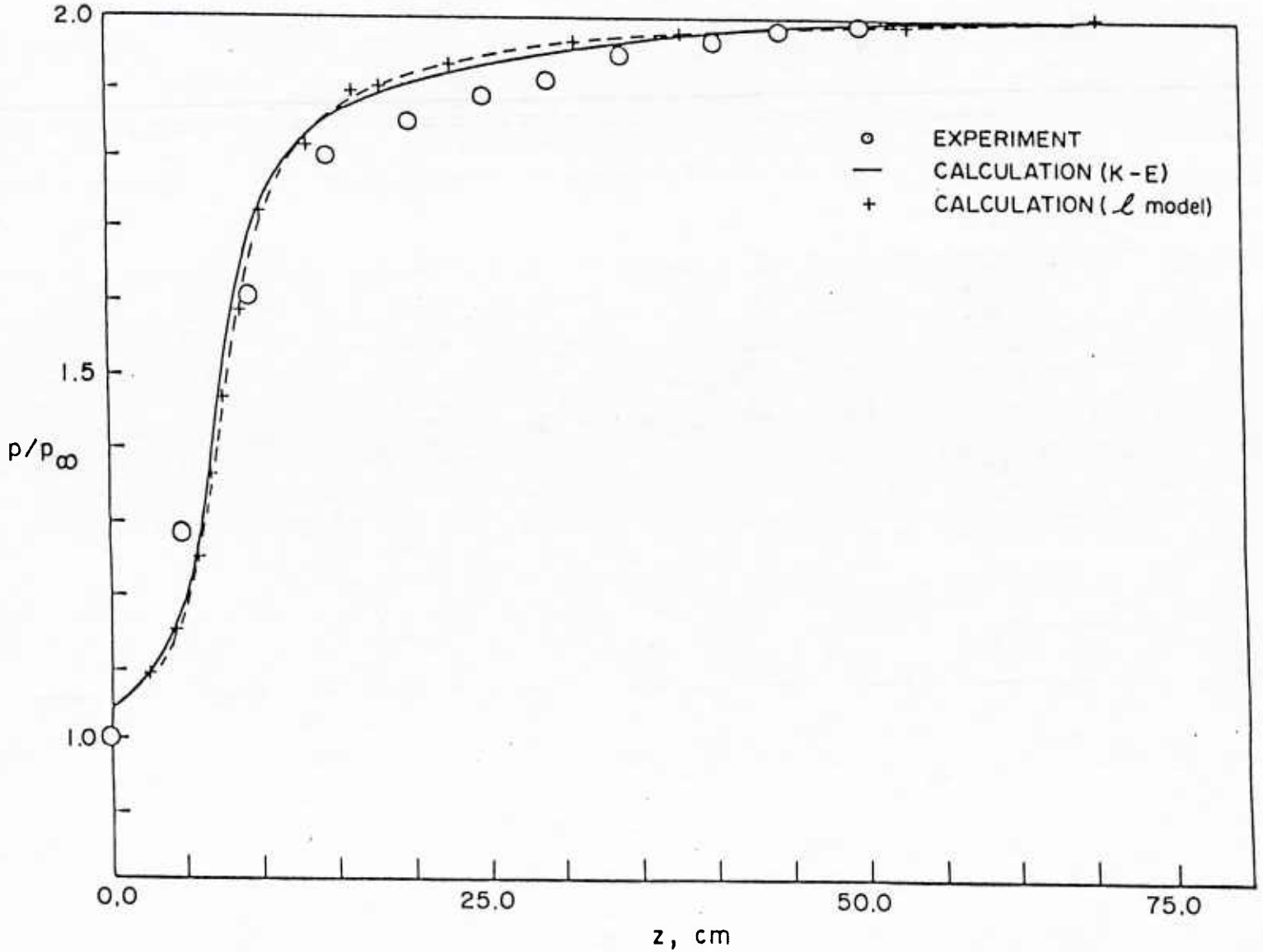


Fig. 3 - Wall static pressure distribution - normal shock in tube.

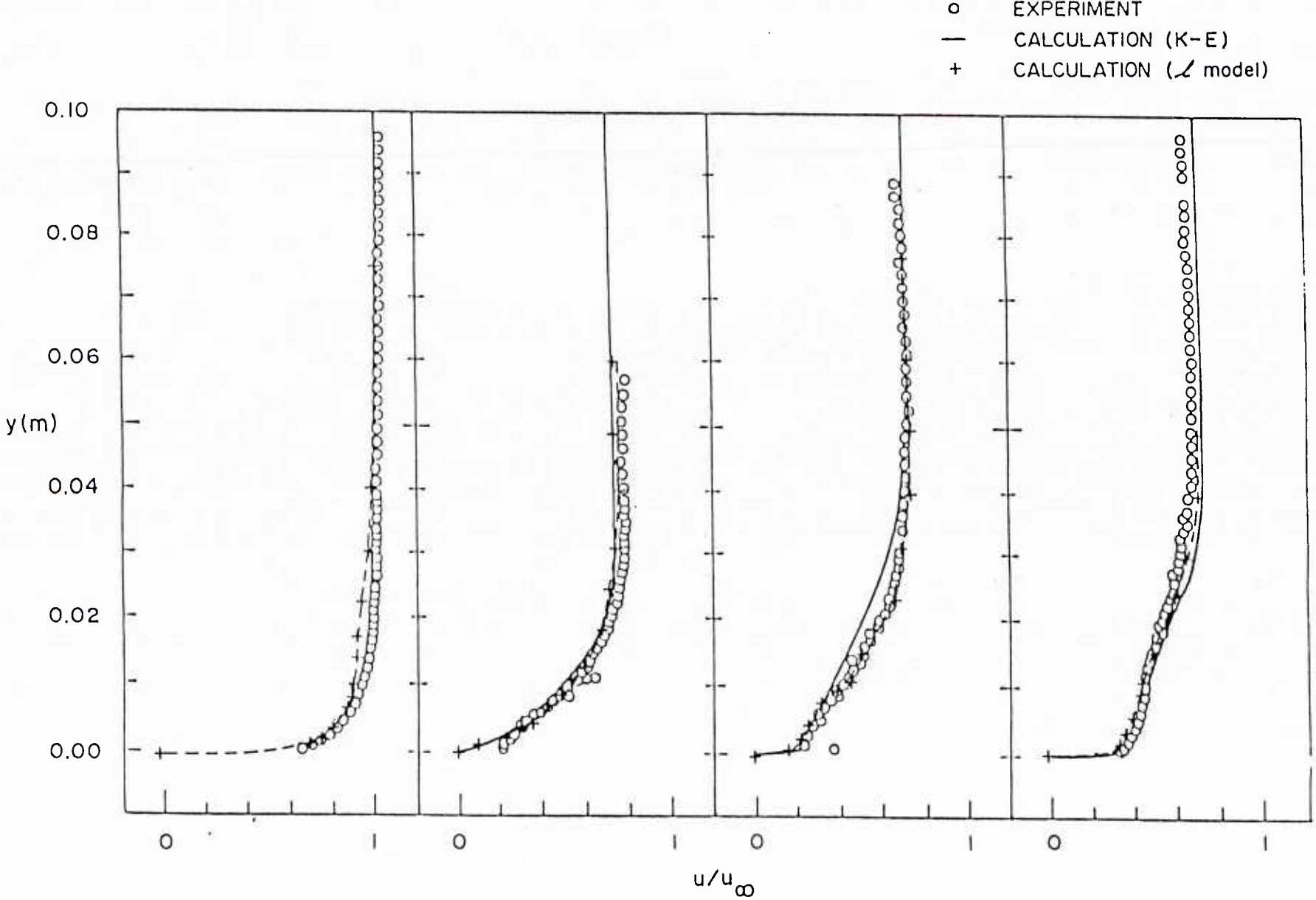


Fig. 4 - Velocity profile - normal shock in tube.

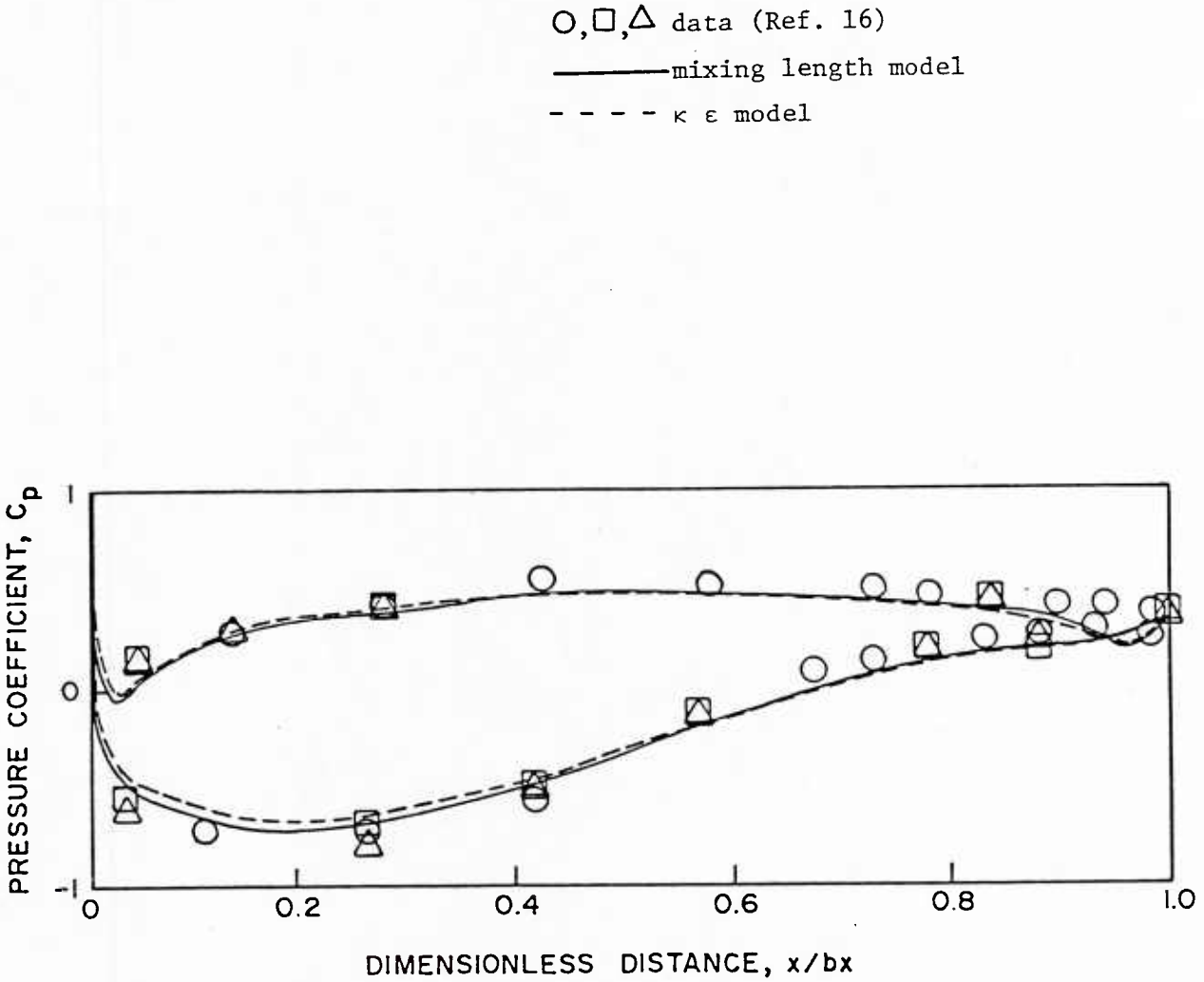


Fig. 5 - Airfoil surface pressure distribution for Hobbs Cascade.

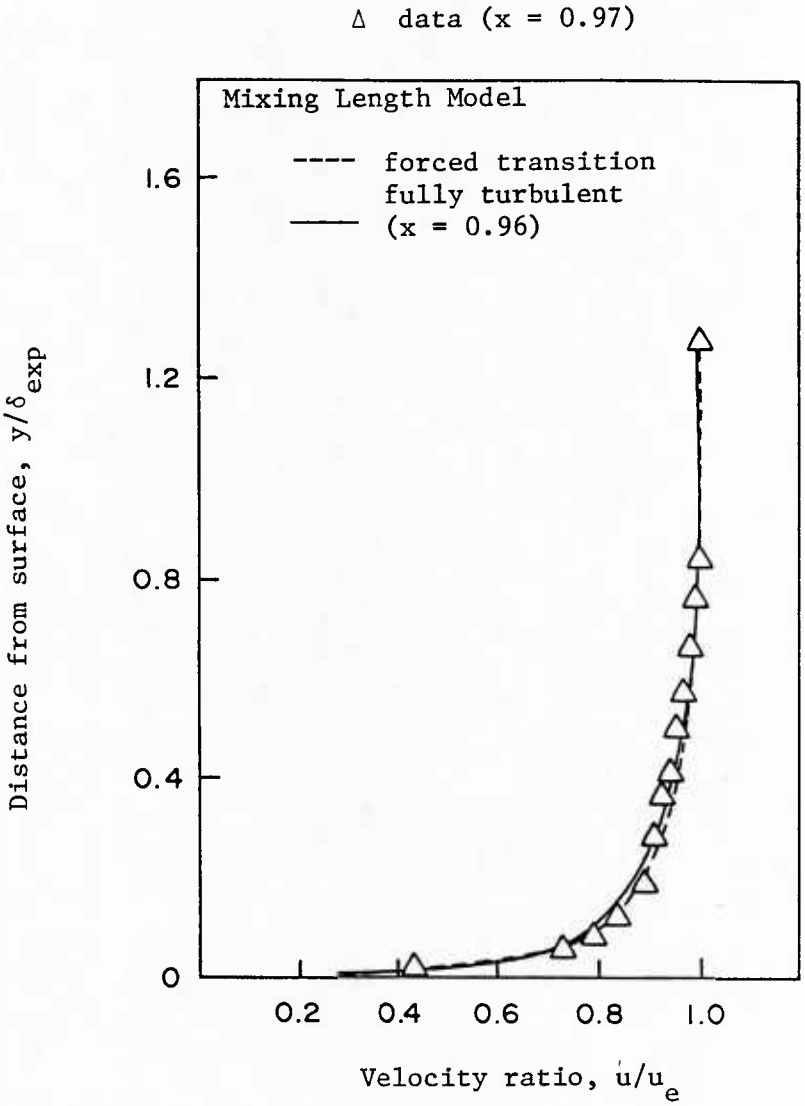


Fig. 6 - Pressure surface boundary layer profile for Hobbs cascade.

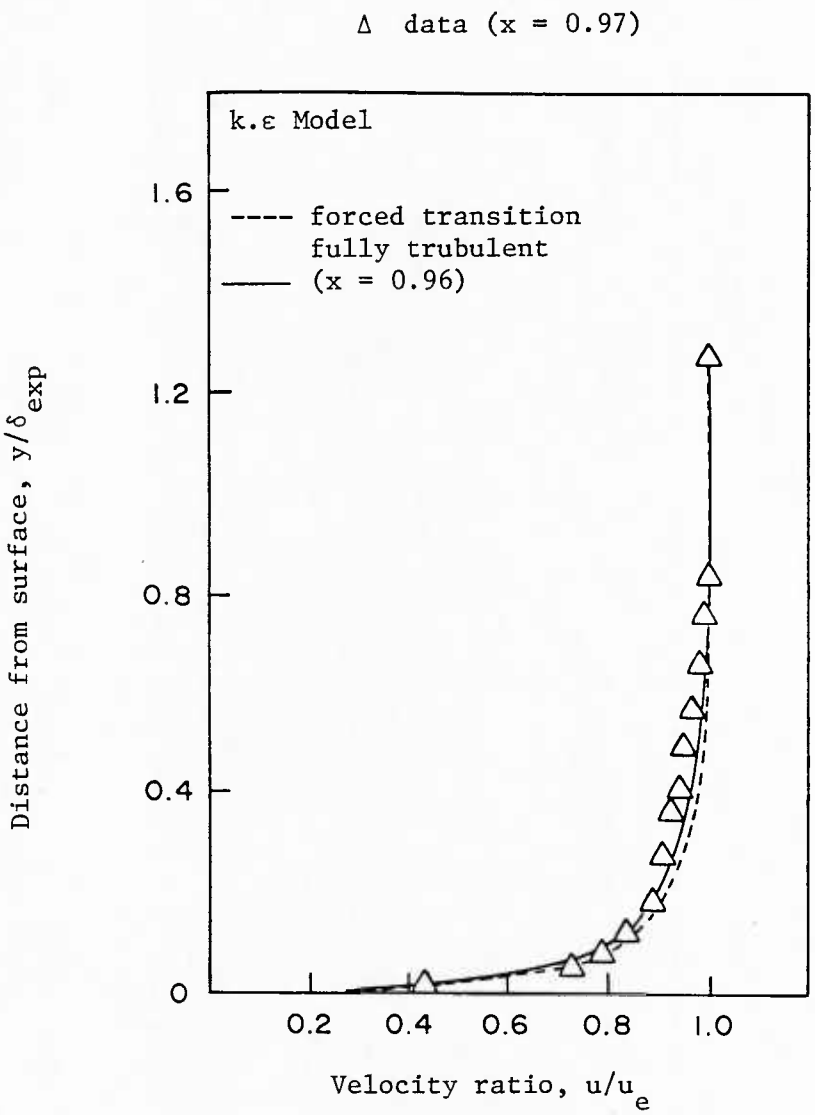


Fig. 7 - Pressure surface boundary layer profile for Hobbs cascade.

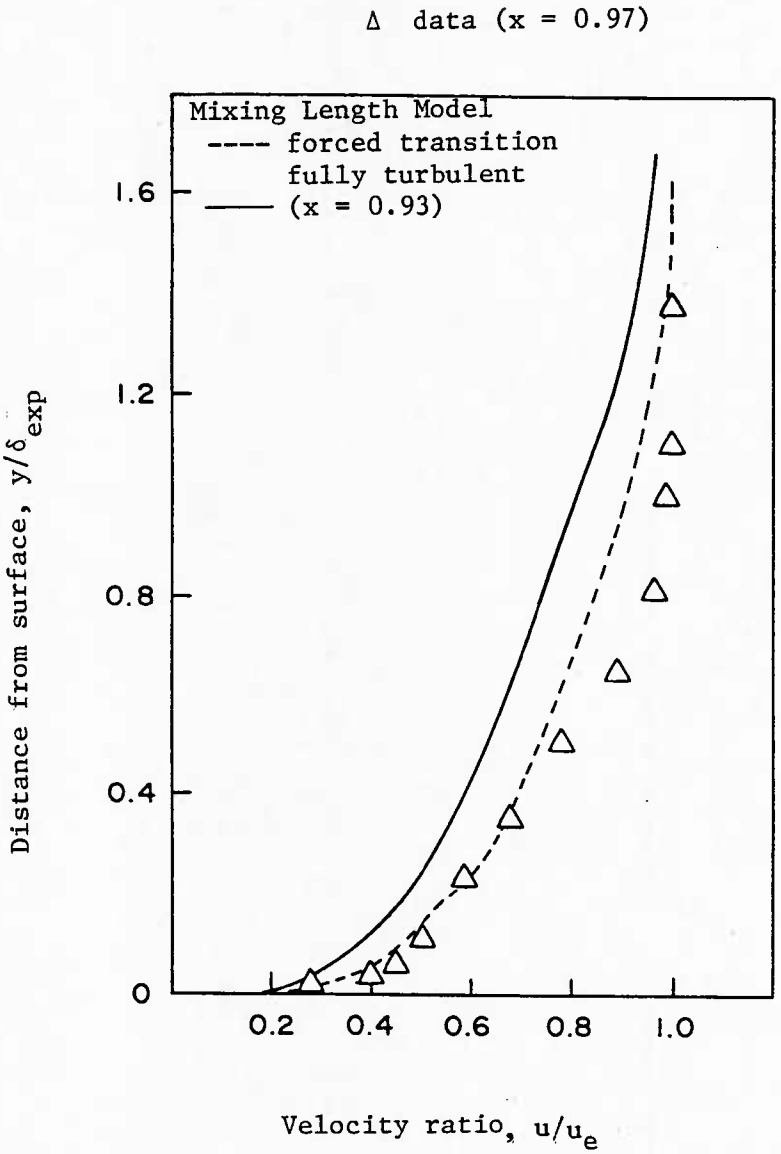


Fig. 8 - Suction surface boundary layer profile for Hobbs cascade.

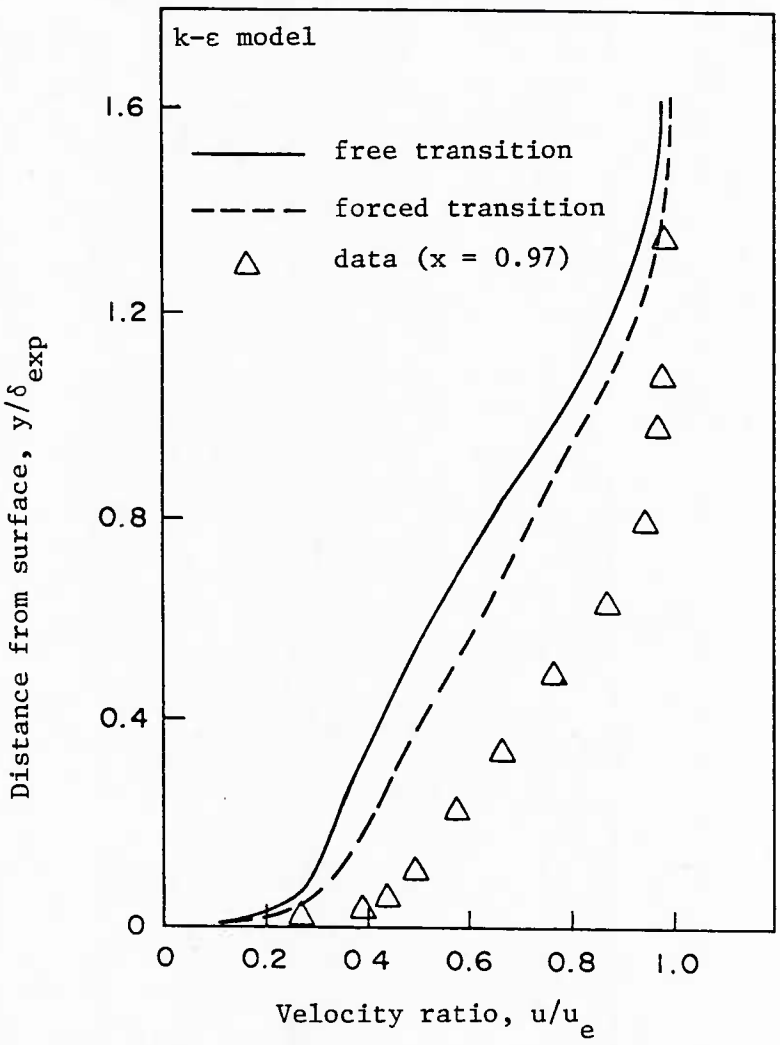


Fig. 9 - Suction surface boundary layer profile for Hobbs cascade.

## APPENDIX A - COORDINATE SYSTEM GENERATION

In brief, the coordinate system consists of a set of two families of curves; the $\xi$ = constant curves such as lines FG or HI in Fig. 1 and the $\eta$ = constant curves such as ABCD or A'ED' in Fig. 1. The coordinate system is constructed by first forming the inner loop A'ED' which includes the blade. The blade may be either specified by an analytic equation or by discrete data points. If an equation is used, then construction of the inner loop is straight-forward. If the blade is specified by discrete data points, then, in general, the points required on the inner loop will not coincide with any point used for blade specification. In this case, a curve fit is used to obtain the required inner loop points. The curve fit used is based upon a local parabolic fit. For any given point required on the inner loop, a parabola is fit through three adjacent specifying points, two on the right and one on the left. A second parabola is then fit through the two points on the left and one on the right. The location of the required point is obtained via a weighted average of these curve fits with the weighting factor being determined by the distance from the required point to the center specifying point of each parabola. This is followed by constructing an outer loop ABCD which consists of periodic lines AB and CD and a frontal curve BC. Both the inner and outer loops are then represented by parametric curves

$$x = x(s), \quad y = y(s)$$

where the parameter varies from zero to unity. The present coordinate generation process utilizes a multi-part transformation. First x and y are expressed as a function of s', the physical distance along the curve. Then s' is related to s via a hyperbolic tangent parametrization centered about the leading edge for the inner loop, and a cubic polynomial representation for the outer loop. The inner loop transformation parametric representation is chosen so as to have rapid variation in the airfoil leading edge region. Both the inner loop hyperbolic tangent transformation and the outer loop cubic transformation are performed between s'/2 and 0 and between s'/2 and s' on each loop. This ensures that the distance in transformed space s between any point on the upper periodic line, line AB, and point A is the same as the distance in transformed space between the corresponding point on the lower periodic line,

line CD, and point D. Similarly, corresponding points on the branch cut will be equi-distant in s from the branch cut end points, points A' and D'. This property is required if corresponding branch cut points (and corresponding periodic line points) are to fall on the same pseudo-radial line.

If N pseudo-radial lines are to be used, the grid points on each loop are chosen at values

$$s_i = (i-1)/(N-1) \qquad i = 0,\ N-1$$

and points having the same value of $s_i$ on the inner and outer loops define the end points for a given pseudo-radial line (e.g. HI). Since the loops are parameterized so that s varies rapidly in the region of the leading edge, this process effectively packs points into the leading edge region. These points are then connected via cubic curve polynomials which allow specification of the slope at each end point (Ref. 7, SRA Rpt.). For pseudo-radial lines which intersect the inner loop downstream of a user specified location (usually $x/c < .05$), the slopes are specified so as to be vertical or normal at the inner loop end points. For pseudo-radial lines whose intersection with the inner loop is upstream of this location a smooth variation of the angle to the horizontal with distance around the leading edge is specified. With this process, the pseudo-radial lines are vertical as they pass through the periodic lines (BA and CD) and, therefore, the metric data will be continuous across these lines. This process allows construction of all pseudo-radial lines.

The second set of coordinate lines, the pseudo-azimuthal lines (e.g. JPK) are obtained by normalizing the length along each line with a hyperbolic tangent transformation that packs points near the airfoil surface (or branch cut). Then if M pseudo-azimuthal lines are to be used, the grid point for the $j^{th}$ pseudo-azimuthal point occurs at $r_j = (j-1)/(M-1)$ for each pseudo-radial line. The actual systems used in the present effort consisted of 113 points along each loop and 30 points along each pseudo-radial line. The plot shown in Fig. 1 is a computer generated plot for the Jose Sanz cascade in which all grid points are not included. For clarity, radial lines in the vicinty of the leading edge were omitted and loops in the vicinity of the blade surface were omitted, leading to the non-smooth appearance of the grid.

The actual grid spacing normal to the surface was $4 \times 10^{-5}$ chords at the blade surface and the spacing along the blade surface was $4.6 \times 10^{-3}$ chords at the blade leading edge. In addition, the grid extended two chords downstream of the airfoil trailing edge.

In generating the coordinate system, it is usually necessary to adjust the parameters of the inner and outer loop transformation to control the location of the pseudo-radial lines, to maintain a smooth variation of metric data and to minimize coordinate nonorthogonality. In some cases it may be necessary to add additional parameterizations to provide a suitable grid. In general, the additional transformations used are local transformations which only affect specific regions of the loops. For example, if it is desired to increase the parametric variation between points A and B, then

$$S' = S \qquad S \leq S_A$$

$$S' = S + \frac{\epsilon}{2}\left[1 - \cos(\pi (S - S_A)/(S_B - S_A))\right] \qquad S_A < S < S_B$$

$$S' = S + \epsilon \qquad S \geq S_B$$

would be a suitable local transformation.

## APPENDIX B - SOLUTION PROCEDURE [23]

### Background

The solution procedure employs a consistently-split linearized block implicit (LBI) algorithm which has been discussed in detail in [12, 21]. There are two important elements of this method:

(1) the use of a noniterative formal time linearization to produce a fully-coupled linear multidimensional scheme which is written in "block implicit" form; and

(2) solution of this linearized coupled scheme using a consistent "splitting" (ADI scheme) patterned after the Douglas-Gunn [22] treatment of scalar ADI schemes.

The method is thus referred to as a split linearized block implicit (LBI) scheme. The method has several attributes:

(1) the noniterative liearization is efficient;

(2) the fully-coupled linearized algorithm eliminates instabilities and/or extremely slow convergence rates often attributed to methods which employ ad hoc decoupling and linearization assumptions to identify nonlinear coefficients which are then treated by lag and update techniques;

(3) the splitting or ADI technique produces an efficient algorithm which is stable for large time steps and also provides a means for convergence acceleration for further efficiency in computing steady solutions;

(4) intermediate steps of the splitting are consistent with the governing equations, and this means that the "physical" boundary conditions can be used for the intermediate solutions. Other splittings which are inconsistent can have several difficulties in satisfying physical boundary conditions [21].

(5) the convergence rate and overall efficiency of the algorithm are much less sensitive to mesh refinement and redistribution than algorithms based on explicit schemes or which employ ad hoc decoupling and linearization assumptions. This is important for accuracy and for computing turbulent flows with viscous sublayer resolution; and

(6) the method is general and is specifically designed for the complex systems of equations which govern multiscale viscous flow in complicated geometries.

This same algorithm was later considered by Beam and Warming [36], but the ADI splitting was derived by approximate factorization instead of the Douglas-Gunn procedure. They refer to the algorithm as a "delta form" approximate factorization scheme. This scheme replaced an earlier non-delta form scheme [37], which has inconsistent intermediate steps.

## Spatial Differencing and Artificial Dissipation

The spatial differencing procedures used are a straightforward adaption of those used in [12] and elsewhere. Three-point central differene formulas are used for spatial derivatives, including the first-derivative convection and pressure gradient terms. This has an advantage over one-sided formulas in flow calculations subject to "two point" boundary conditions (virtually all viscous or subsonic flows), in that all boundary conditions enter the algorithm implicitly. In practical flow calculations, artificial dissipation is usually needed and is added to control high-frequency numerical oscillations which otherwise occur with the central-difference formula.

In the present investigation, artificial (anisotropic) dissipation terms of the form

$$\sum_j \frac{d_j}{h_j^2} \frac{\partial^2 u_k}{\partial x_j^2} \tag{1}$$

are added to the right-hand side of each (k-th) component of the momentum equation, where for each coordinate direction $x_j$, the artificial diffusivity $d_j$ is positive and is chosen as the larger of zero and the local quantity $\mu_e$ $(\sigma\ Re_{\Delta x}-1)/Re$. Here, the local cell Reynolds number $Re_{\Delta xj}$ for the j-th direction is defined by

$$Re_{\Delta x_j} = Re \left|\rho u_j\right| \Delta x_j / \mu_e \tag{2}$$

This treatment lowers the formal accuracy to 0 ($\Delta x$), but the functional form is such that accuracy in representing physical shear stresses in thin shear layers with small normal velocity is not seriously degraded. This latter

property follows from the anisotropic form of the dissipation and the combination of both small normal velocity and small grid spacing in thin shear layers.

## Split LBI Algorithm

### Linearization and Time Differencing

The system of governing equations to be solved consists of three/four equations: continuity and two/three components of momentum equation in three/four dependent variables: $\rho$, u, v, w. Using notation similar to that in [12], at a single grid point this system of equations can be written in the following form:

$$\partial H(\phi)/\partial t = D(\phi) + S(\phi) \tag{3}$$

where $\phi$ is the column-vector of dependent variables, H and S are column-vector algebraic functions of $\phi$, and D is a column vector whose elements are the spatial differential operators which generate all spatial derivatives appearing in the governing equation associated with that element.

The solution procedure is based on the following two-level implicit time-difference approximations of (3):

$$(H^{n+1} - H^n)/\Delta t = \beta(D^{n+1} + S^{n+1}) \quad (1-\beta)\,(D^n + S^n) \tag{4}$$

where, for example, $H^{n+1}$ denotes $H(\phi^{n+1})$ and $\Delta t = t^{n+1} - t^n$. The parameter $\beta$ ($0.5 \leq \beta \leq 1$) permits a variable time-centering of the scheme, with a truncation error of order $[\Delta t^2, (\beta - 1/2)\,\Delta t]$.

A local time linearization (Taylor expansion about $\phi^n$) of requisite formal accuracy is introduced, and this serves to define a <u>linear</u> differential operator L (cf. [12]) such that

$$D^{n+1} = D^n + L^n(\phi^{n+1} - \phi^n) + O(\Delta t^2) \tag{5}$$

Similarly,

$$H^{n+1} = H^n + (\partial H/\partial \phi)^n\,(\phi^{n+1} - \phi^n) + O\,(\Delta t^2) \tag{6}$$

$$S^{n+1} = S^n + (\partial S/\partial \phi)^n\,(\phi^{n+1} - \phi^n) + O\,(\Delta t^2) \tag{7}$$

Eqs. (5-7) are inserted into Eq. (4) to obtain the following system which is linear in $\phi^{n+1}$

$$(A - \beta\Delta t\, L^n)\,(\phi^{n+1} - \phi^n) = \Delta t\,(D^n + S^n) \tag{8}$$

and which is termed a linearized block implilcit (LBI) scheme. Here, A denotes a matrix defined by

$$A \equiv (\partial H/\partial \phi)^n - \beta \Delta t \, (\partial S/\partial \phi)^n \tag{9}$$

Eq. (8) has 0 ($\Delta t$) accuracy unless $H \equiv \phi$, in which case the accuracy is the same as Eq. (4).

Special Treatment of Diffusive Terms

The time differencing of diffusive terms is modified to accomodate cross-derivative terms and also turbulent viscosity and artificial dissipation coefficients which depend on the solution variables. Although formal linearization of the convection and pressure gradient terms and the resulting implicit coupling of variables is critical to the stability and rapid convergence of the algorithm, this does not appear to be important for the turbulent viscosity and artificial dissipation coefficients. Since the relationship between $\mu_e$ and $d_j$ and the mean flow variables is not conveniently linearized, these diffusive coefficients are evaluated explicitly at $t^n$ during each time step. Notationally, this is equivalent to neglecting terms proportional to $\partial \mu_e/\partial \phi$ or $\partial d_j/\partial \phi$ in $L^n$, which are formally present in the Taylor expansion (5), but retaining all terms proportional to $\mu_e$ or $d_j$ in both $L^n$ and $D^n$.

It has been found through extensive experience that this has little if any effect on the performance of the algorithm. This treatment also has the added benefit that the turbulence model equations can be decoupled from the system of mean flow equations by an appropriate matrix partitioning (cf. [21]) and solved separately in each step of the ADI solution procedure. This reduces the block size of the block tridiagonal systems which must be solved in each step and thus reduces the computational labor.

In addition, the viscous terms in the present formulation include a number of spatial cross-derivative terms. Although it is possible to treat cross-derivative terms implicitly within the ADI treatment which follows, it is not at all convenient to do so; and consequently, all cross-derivative terms are evaluated explicitly at $t^n$. For a scalar model equation representing combined convection and diffusion, it has been shown by Beam and Warming [38] that the explicit treatment of cross-derivative terms does not degrade the unconditional stability of the present algorithm. To preserve notational simplicity, it is understood that all cross-derivative terms appearing in $L^n$ are neglected but are retained in $D^n$. It is important to

note that neglecting terms in $L^n$ has no effect on steady solutions of Eq. (8), since $\phi^{n+1} - \phi^n \equiv 0$, and thus Eq. (8) reduces to the steady form of the equations: $D^n + S^n = 0$. Aside from stability considerations, the only effort of neglecting terms in $L^n$ is to introduce an 0 ($\Delta t$) truncation error.

Consistent Splitting of the LBI Scheme

To obtain an efficient algorithm, the linearized system (8) is split using ADI techniques. To obtain the split scheme, the multidimensional operator L is rewritten as the sum of three "one-dimensional" sub-operators $L_i$ (i = 1, 2, 3) each of which contains all terms having derivatives with respect to the i-th coordinate. The split form of Eq. (8) can be derived either as in [12, 21] by following the procedure described by Douglas and Gunn [22] in their generalization and unification of scalar ADI schemes, or using approximate factorization. For the present system of equations, the split algorithm is given by

$$(A - \beta\Delta t L_1^n)\ (\phi^* - \phi^n) = \Delta t\ (D^n + S^n) \tag{10a}$$

$$(A - \beta\Delta t L_2^n)\ (\phi^{**} - \phi^n) = A\ (\phi^* - \phi^n) \tag{10b}$$

$$(A - \beta\Delta t L_3^n)\ (\phi^{n+1} - \phi^n) = A\ (\phi^{**} - \phi^n) \tag{10c}$$

where $\phi^*$ and $\phi^{**}$ are consistent intermediate solutions. If spatial derivatives appearing in $L_i$ and D are replace by three-point difference formulas, as indicated previously, then each step in Eqs. (10a-c) can be solved by a block-tridiagonal elimination.

Combining Eqs. (10a-c) gives

$$(A - \beta\Delta t L_1^n)\ A^{-1}\ (A - \beta\Delta t L_2^n)\ A^{-1}\ (A - \beta\Delta t L_3^n)\ (\phi^{n+1} - \phi^n) = \Delta t\ (D^n + S^n) \tag{11}$$

which approximates the unsplit scheme (8) to 0 ($\Delta t^2$). Since the intermediate steps are also consistent approximations for Eq. (8), physical boundary conditions can be used for $\phi^*$ and $\phi^{**}$ [12, 21]. Finally, since the $L_i$ are homogeneous operators, it follows from Eqs. (10a-c) that steady solutions have the property that $\phi^{n+1} = \phi^* = \phi^{**} = \phi^n$ and satisfy

$$D^n + S^n = 0 \tag{12}$$

The steady solution thus depends only on the spatial difference approximations used for (12), and does not depend on the solution algorithm itself.